Accurate V_p:V_s relationship for dry consolidated sandstones

Christoph H. Arns,[1] Mark A. Knackstedt,[1,2] and W. Val Pinczewski[1]

Received 18 July 2001; revised 8 October 2001; accepted 12 November 2001; published 20 April 2002.

[1] We use a finite element method to study the elastic properties of dry sandstone morphologies. We show that the dry Poisson's (V_p/V_s) ratio becomes independent of the Poisson's ratio of the solid phase at a critical porosity and that this limiting behaviour holds for any number of solid phases and is insensitive to the manner in which the phases are distributed. We represent the behaviour of the Poisson's ratio as a simple flow diagram and present an empirical structure-property relationship that holds for all Sandstone Morphologies independent of the number of phases and the Poisson's ratio of the solid phase. *INDEX TERMS:* 5102 Physical Properties of Rocks: Acoustic properties; 5112 Physical properties of Rocks: Microstructure; 3230 Mathematical Geophysics: Numerical solutions

1. Introduction

[2] Impedance ratios or V_p/V_s are used for determining lithology from seismic or sonic log data and for direct seismic detection of pore fluids. In actual practice, the shear wave velocity, V_s, is usually not known and must therefore be estimated from the known compressional wave velocity, V_p. A common approach is to estimate V_s from empirical V_p–V_s relationships or models. Examples include Krief's relation [*Krief et al.*, 1990] and the critical porosity model of [*Nur et al.*, 1991, 1995] for consolidated sands and the models of [*Digby*, 1981; *Winkler*, 1983; *Palciauskas*, 1992] for poorly consolidated rocks. The empirical relationships of Krief and Nur for dry sands exhibit the same dependence on porosity for both the bulk and shear modulus, trending toward the value for the solid mineral in the limit of zero porosity and toward zero in the limit of a critical porosity, ϕ_c. This is equivalent to assuming that the dry rock V_p/V_s or Poisson's ratio, ν, is independent of porosity, ϕ, and equal to the solid $(V_p/V_s)_s$ or ν_s. [*Digby*, 1981; *Winkler*, 1983; *Palciauskas*, 1992] predict a ν which is independent of porosity, but assume that it is only weakly dependent on the solid mineral ν_s; these models, derived for poorly consolidated rocks, predict $\nu \simeq 0.14$ or $V_p/V_s \simeq 1.55$ for all ϕ.

[3] Experimental measurements of Poisson's ratio are notoriously noisy. This scatter can be due to lithology (pore shape, size, degree of compaction) and in particular, clay content and distribution. We use numerical simulations to calculate the elastic properties of model rock morphologies. Due to the ability to control pore space structure and rock mineralogy within a numerical model, resultant data sets exhibit much less noise than experimental data and one can quantitatively analyze the effects of ϕ and the mineral phase modulus on the resultant elastic properties. We use numerical calculations to show that ν is in fact a non-linear function of ϕ and that it trends from the value for the solid mineral in the limit of zero porosity to a constant value of $\nu = 0.2$, $V_p/V_s = 1.63$, at porosity $\phi_c = 0.5$, independent of mineral type. This limit is shown to be true for clean (monomineralic) sands and for model sands containing cements (multiple-mineral phases). We present a simple universal predictive equation for dry sands which holds for all the systems simulated, irrespective of the number of mineral phases present or the Poisson's ratio of the solid mineral.

[1]School of Petroleum Engineering, University of New South Wales, Sydney, Australia.

[2]Department of Applied Mathematics, Research School of Physical Sciences and Engineering, Australian National University, Canberra, Australia.

0094-8276/02/2001GL013788

2. Poisson's Ratio for Sandstone Morphology

[4] A natural statistical model for a consolidated sandstone is based on an overlapping spherical grain (OS) morphology [*Thovert et al.*, 2001; *Arns et al.*, 2001a, 2001b]. The OS morphology is shown in Figure 1a. In recent work we used a finite-element method [*Garboczi and Day*, 1995] to derive modulus/porosity relationships directly from microtomographic images for a suite of Fontainebleau sandstone - a clean, homogeneous, consolidated sandstone, composed of quartz grains with quartz cement and displaying only intergranular porosity. The numerically derived properties were in excellent agreement with experimental measurements on Fontainebleau [*Han*, 1986] over the entire range of the porosity sampled. Unfortunately the number of data sets available for numerical study via microtomography is limited. The same numerical property calculations can however be performed on model rock morphologies. Elastic calculations for an OS morphology with pure quartz grains are in agreement with the Fontainebleau data. This suggests that the OS morphology accurately describes the microstructure of homogeneous sandstones. We use this idealized morphology to study the behaviour of the Poisson's ratio for dry sandstones across a wide range of porosity.

2.1. Clean Sandstones

[5] We first study the behaviour for clean sandstones; we consider two single mineral phases, quartz (q) and feldspar (f), having different ν_s. The properties of these minerals were taken from tables in [*Mavko et al.*, 1998] (for quartz - $K_q = 37.0$ GPa, $\mu_q = 44.0$ GPa and $\nu_s^q = 0.08$ and for feldspar - $K_f = 37.5$ GPa, $\mu_f = 15.0$ GPa and $\nu_s^f = 0.32$). The numerical predictions for the Poisson's ratio of the quartz and feldspar systems are plotted in Figure 2.

[6] Two striking features in the data sets are immediately evident. First is the lack of noise in the data sets when compared to typical experimental results (see e.g., [*Han*, 1986]). The standard error in the data is extremely small < 1% for most measurements. Only for V_p/V_s at high porosities does the standard error exceed a few percent. Importantly, the numerical data in the region of most interest, $5\% < \phi < 25\%$, exhibits much less noise than typical experimental data. The ability to control the pore space structure, microstructure and mineralogy of the material within a numerical model as well as the ability to average over a large number of statistically identical samples allows one to generate effectively noiseless data which, although based on an idealized microstructure, will allow us to *quantitatively* analyze the effects of porosity and the elastic properties of the mineral phase. The second feature in the plot is that the Poisson's ratio for the model morphology becomes independent of the Poisson's ratio for the mineral solid at a critical porosity. In both cases, despite very different values of mineral ν_s, the flow diagram for $\nu(\phi, \nu_s)$ converges to a fixed point at $\phi_c \simeq 0.5$. This result has previously been observed both numerically [*Day et al.*, 1992] and analytically [*Cherkaev et al.*,

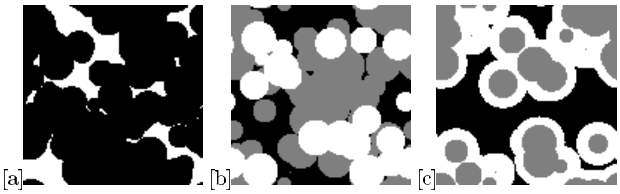

Figure 1. Images of the pore space of an OS morphology. (a) 2D slice through a 3D representation of the single mineral model microstructure (black phase) at a porosity of 20%. (b) framework and (c) interstitial two phase mineral models are illustrated at a mineral ratio of 1:1 and a porosity of 20%. The first mineral phase is gray, the second mineral is white. The image size is the same as considered in the simulations, $(120)^3$, and the spheres have radius $r = 12$.

1992; *Thorpe and Jasiuk*, 1992] for *two*-dimensional dry porous materials composed of a single solid mineral. The critical porosity in 2D was thought to coincide with the geometric (percolation) threshold $\phi^* = 0.5$ [*Day et al.*, 1992]. The percolation threshold for the solid phase of the OS morphology in three dimensions is $\phi^* \simeq 0.8$. It is not clear why the point of convergence of the Poisson's ratio in three-dimensions coincides with the two-dimensional threshold. The experimental data of [*Han*, 1986] for clean quartz sandstones is also plotted. This experimental data follows the numerical prediction of the pure quartz curve for the range of porosities studied.

[7] *Roberts and Garboczi* [2000] have studied the behaviour of the Poisson's ratio for a range of model morphologies. They find, to a reasonable approximation, that ν can be described as a linear function of ϕ and ν_s; $\nu(\nu_s, \phi) = \nu_s + \frac{\phi}{\phi_c}(\nu_c - \nu_s)$. This equation, with $\phi_c = 0.5$ and $\nu_c = 0.2$, gives an improved prediction for the dry rock Poisson's ratio compared to the common empirical estimate that ν is independent of ϕ. However, the plot in Figure 2 exhibits a clear non-linear behaviour. This behaviour is well approximated by the predictive non-linear empirical equation,

$$\nu = \begin{cases} \nu_s + (2\phi)^{1.5}(0.2 - \nu_s) & , \quad \nu_s < 0.2 \\ 0.2 + (1 - 2\phi)^{1.5}(\nu_s - 0.2) & , \quad \nu_s > 0.2. \end{cases} \qquad (1)$$

This equation provides an excellent fit to the data of Figure 2.[1]

2.2. Cemented Sandstones

[8] Sandstones are rarely clean, frequently containing varying amounts of clay and cements, which can affect their elastic properties. These minerals can be distributed in a number of ways in the rock framework depending on the conditions at deposition, on compaction, bioturbation and diagenesis. One would expect the Poisson's ratio for cemented sandstones to depend on the properties and volume fractions f_i of the i components of the solid matrix mineralogy, i.e. $\nu = \nu(\phi, \nu_s^i, f^i)$. We consider two model microstructures for cemented sands; a structural or framework cement/sand mix, and a dispersed or interstitial cement/sand mixture. The framework microstructure is based on the placement of spheres of mineral phase 1, and then overgrowth by placement of identical permeable spheres of mineral phase 2. The interstitial microstructure is based on an OS morphology for the first mineral phase and allows overgrowth of the second mineral phase into the pore space by parallel surfaces. Figures 1b and 1c shows the morphological differences between the two cementation schemes.

[9] We consider model rock morphologies with different ratios of quartz to cement, including 1:4, 1:2, 1:1, 2:1 and 4:1. The

[1]We note that the self-consistent approximation (SCA) (see e.g., [*Mavko et al.*, 1998]) does give the correct limiting behavior, $\phi_c = 0.5$, $\nu_c = 0.2$, but the fit to the data is not consistent for both minerals (Figure 2).

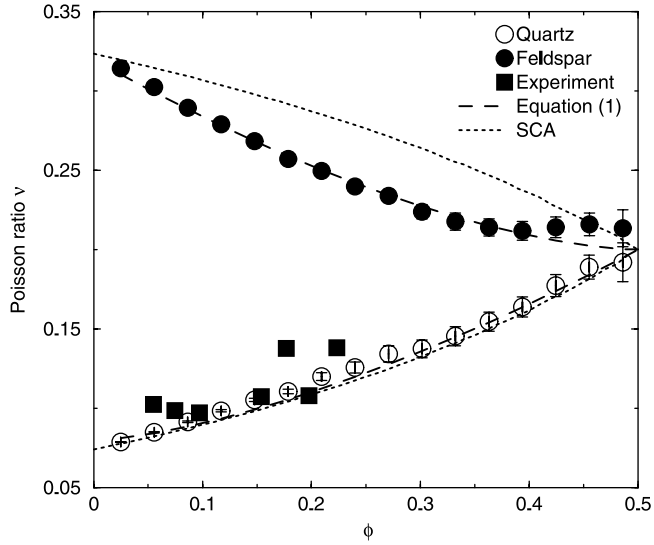

Figure 2. The Poisson's ratio of the OS morphology as a function of porosity for clean dry quartz ($\nu_s = 0.08$) and feldspar ($\nu_s = 0.32$) sands. The Poisson's ratio of both systems goes to $\nu^* = 0.2$ as $\phi \rightarrow 0.5$. Standard error bars are shown and are of the order of the size of the data point. The experimental data of [*Han*, 1986] for clean quartz sandstones is also shown. The match of the numerical prediction to the experiment is good and the fit of Equation (1) to the data is excellent. The fit of SCA is poor for feldspar.

cementing minerals used in the simulation are dolomite and clay. The values of the elastic properties are for dolomite - $K_d = 69.4$ GPa, $\mu_d = 51.6$ GPa and $\nu_s^d = 0.202$, and for clay $K_c = 20.8$ GPa, $\mu_c = 6.9$ GPa and $\nu_s^c = 0.351$ [*Mavko et al.*, 1998]. The effective solid

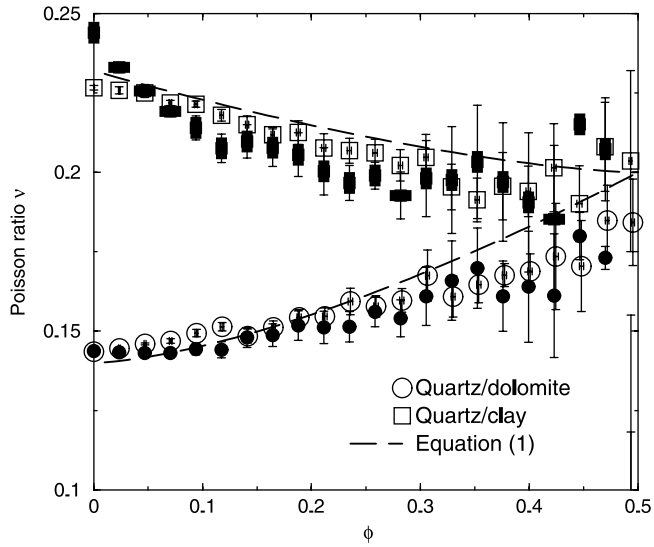

Figure 3. The Poisson ratio for a symmetric 1:1 mixture of quartz/clay and quartz/dolomite. The filled symbols give the numerical results for the interstitial morphology and the open symbols the results on the framework morphology. We show also the characteristic standard errors in the numerical calculation for systems of mixed mineralogy. While they remain small for $\phi < 0.30$, they can diverge for some morphologies at higher porosities. The flow diagram still converges to a fixed point at $\phi_c \simeq 0.5$. and seems independent of the cement deposition microstructure. Agreement with empirical Equation (1) is good for both morphologies.

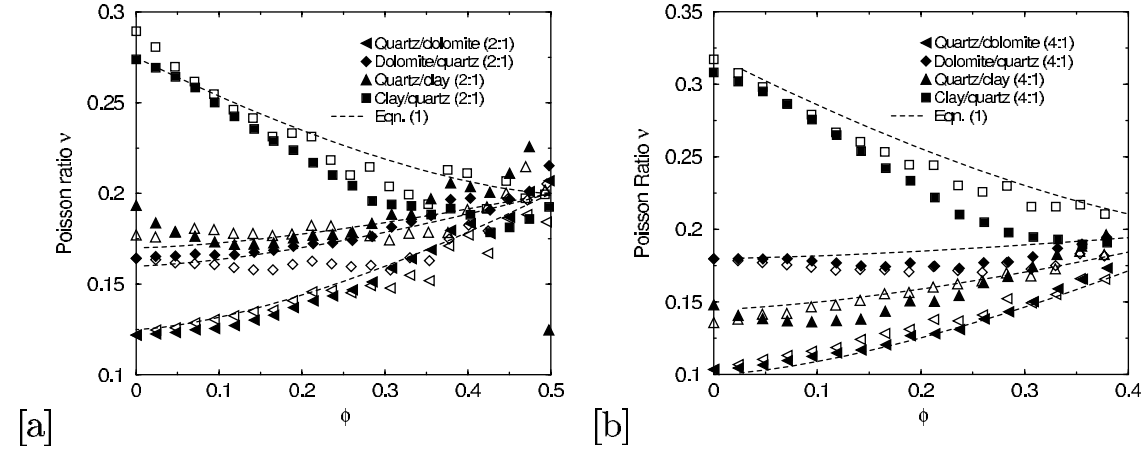

Figure 4. The Poisson ratio for asymmetric 2:1 and 4:1 mixtures of quartz/clay and quartz/dolomite. Symbols are the same as in Figure 3. Agreement with empirical Equation (1) is good for both morphologies at all mineral ratios.

Poisson's ratio ν_s for the two phase mineral mixtures, is determined numerically.

[10] Figure 3 shows the numerical prediction of the Poisson's ratio for quartz/clay and quartz/dolomite systems at a 1:1 volume ratio. The numerical data for the mixed mineralogy microstructure is noisier than for monomineralic systems indicating larger numerical errors, but the trend in the data is still clear. In all cases, despite very different values of ν_s^i, the flow diagram for $\nu(\phi, f_s^i, \nu_s^i)$ converges to the fixed point $\nu \rightarrow 0.2$ at $\phi_c \simeq 0.5$ - the same limit observed for the monomineralic system. The empirical equation developed for clean sandstones, Equation (1), again provides a good fit for the mixed mineralogy system. Interestingly, the distribution of the phases (intergranular deposition versus surface deposition) has little effect on the computed Poisson's ratio. This is *not* generally observed for other mechanical properties [*Knackstedt et al.*, 2001]. The result is consistent with measured data which indicate that the V_p/V_s ratio is mostly insensitive to the presence and distribution of clays [*Mavko et al.*, 1998].

[11] Similar results are obtained for a wider range of quartz/clay and quartz/dolomite ratios. Figures 4a–4b shows the numerical predictions for ratios of 2:1 and 4:1 for both depositional microstructures. Again, in all cases, the flow diagram for $\nu(\phi, f_s^i, \nu_s^i)$ converges to the fixed point $\nu \rightarrow 0.2$ at $\phi_c \simeq 0.5$ and the fit of the empirical Equation (1) to the data is still good. The choice of intergranular deposition or surface deposition has little effect on the Poisson's ratio. The results for the interstitial 4:1 model are noisy for porosities $\phi > 0.35$ due to difficulties with numerical discretization of the parallel surfaces. Data for the model up to $\phi = 0.35$ however shows a clear trend towards $\nu \rightarrow 0.2$ for all ν_s chosen. Data for the framework model at the 4:1 ratio converges to $\nu \rightarrow 0.2$.

[12] Comparison of the prediction of Equation (1) to experimental data is shown in Figure 5. We consider the Poisson's ratio data for shaley sandstones from [*Han*, 1986] where we have binned the data into groups of clean, intermediate (< 15%) and higher (15–35%) clay content. We also show laboratory data sets for clay cemented quartz sands from the Oseberg field [*Dvorkin and Nur*, 1996]. The variation with clay content and porosity is consistent with the prediction of Equation (1) and provides a much better fit than other commonly used models; $\nu = \nu_s$ [*Krief et al.*, 1990; *Nur et al.*, 1991], $\nu = 0.14$ [*Digby*, 1981; *Winkler*, 1983; *Palciauskas*, 1992] and $\nu \simeq 0.04$ [*Dvorkin and Nur*, 1996].

[13] We have extended the work to three mineral phases and continue to observe the same limiting behaviour for the Poisson's ratio. We believe that these results indicate that this behaviour of Poisson's ratio is universal for this morphology and that it may be expected to occur for most dry sands. ϕ_c and ν_c may differ however for different rock morphologies [*Roberts and Garboczi*, 2000]. Again, this is consistent with the observation that ϕ_c for the empirical critical porosity model depends on rock type [*Mavko et al.*, 1998].

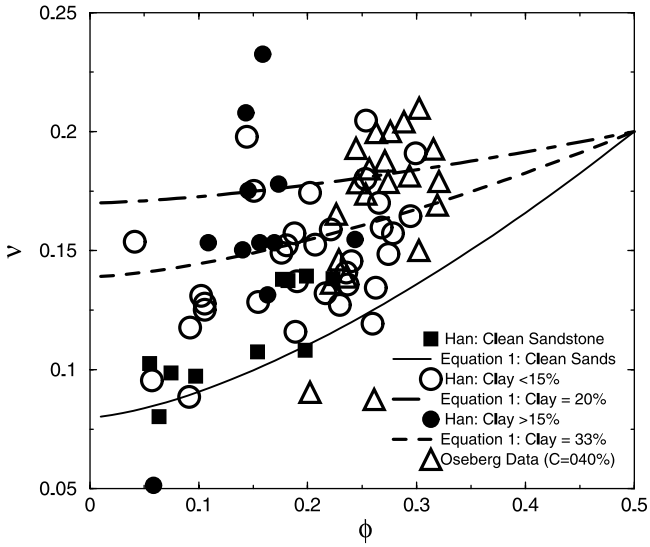

Figure 5. Comparison of data from [*Han*, 1986] and [*Dvorkin and Nur*, 1996] for clay-bearing sands to the prediction of Equation (1). The agreement for clean sands is excellent. Data for systems at finite clay fraction is very noisy, but in general the sands with lower clay fraction are centered about the Q:C = 4:1 line and higher fractions are consistent with the Q:C = 2:1 predictions.

3. Conclusion

[14] Numerical simulations on model morphologies for sandstones containing any number of solid mineral phases show that the Poisson's ratio for the dry system trends in a non-linear manner from the effective solid Poisson's ratio in the limit of zero porosity to a constant value of 0.2 at a critical porosity of $\phi_c = 0.5$ which is independent of the solid Poisson's ratio. A simple empirical

equation, $\nu = \nu(\nu_s, \phi)$, fits the numerical data well, is consistent with experiment and provides a better estimate of dry rock Poisson's ratio than the commonly used estimates.

[15] **Acknowledgments.** MAK and WVP thank the Australian Research Council and Australian Partnership for Advanced Computing (APAC) for financial support. We thank the A.N.U. Supercomputing Facility and APAC for generous allocations of computer time. We thank M. Prasad and a referee for helpful comments.

References

Arns, C. H., M. A. Knackstedt, W. V. Pinczewski, and E. G. Garboczi, Computation of linear elastic properties from microtomographic images: Methodology and agreement with theory and experiment, *Geophysics*, now accepted, 2002.

Arns, C. H., M. A. Knackstedt, W. V. Pinczewski, and K. Mecke, Boolean reconstructions of complex materials: Integral Geometric Approach, *Phys. Rev. E*, submitted, 2001.

Castagna, J. P., M. L. Batzle, and T. K. Kan, Rock physics—the link between rock properties and AVO response, in *Offset-dependent reflectivity—theory and practice of AVO analysis*, edited by J. P. Castagna and M. M. Backus, Society of Exploration Geophysicists, pp. 135–171, 1993.

Cherkaev, A. V., K. A. Lurie, and G. W. Milton, Invariant properties of the stress in plane elasticity and equivalent classes of composites, *Proc. R. Soc. Lond. A*, *438*, 519–529, 1992.

Day, A. R., K. A. Snyder, E. J. Garboczi, and M. F. Thorpe, The elastic moduli of a sheet containing circular holes, *J. Mech. and Phys. of Solids*, *40*, 1031–1051, 1992.

Digby, P. J., The effective elastic moduli of porous granular rocks, *J. Applied Mechanics*, *48*, 803–808, 1981.

Dvorkin, J., and A. Nur, Elasticity of high-porosity sandstones: Theory for two North Sea data sets, *Geophysics*, *61*, 1363–1370, 1996.

Garboczi, E. J., and A. R. Day, An algorithm for computing the effective linear elastic properties of heterogeneous materials: Three-dimensional results for composites with equal phase poisson ratios, *J. Mech. Phys. Solids*, *43*, 1349–1362, 1995.

Han, D.-H., Effects of porosity and clay content on acoustic properties of sandstones and unconsolidated sediments, Ph.D. thesis, University of Stanford, 1986.

Knackstedt, M. A., C. H. Arns, and W. V. Pinczewski, Velocity-porosity relationships: II. Accurate velocity model for cemented sands composed of two mineral phases, *Geophysical Prospecting*, submitted, 2001.

Krief, M., J. Garat, J. Stellingwerff, and J. Ventre, A petrophysical interpretation using the velocities of *p* and *s* waves (full waveform sonic), *The Log Analyst*, *31*, 355–369, 1990.

Mavko, G., T. Mukerji, and J. Dvorkin, The rock physics handbook, Cambridge University Press, Cambridge, 1998.

Nur, A., D. Marion, and H. Yin, Wave velocities in sediments, in *Shear Waves in Marine sediments*, edited by J. Hovem, M. D. Richardson, and R. D. Stoll, pp. 131–140, Kluwer Academic, 1991.

Nur, A., G. Mavko, J. Dvorkin, and D. Gal, Critical porosity: The key to relating physical properties to porosity in rocks, *Proc. 65th Ann. Int. Meeting Soc. Expl. Geophys.*, 878, 1995.

Palciauskas, V. V., Compressional to shear wave velocity ratio of granular rocks: role of rough grain contacts, *Geophys. Res. Lett.*, *19*, 1683–1686, 1992.

Roberts, A. P., and E. J. Garboczi, Elastic properties of model porous ceramics, *J. Amer. Ceramic Society*, *83*, 3041–3048, 2000.

Thorpe, M. F., and I. Jasiuk, New results in the theory of elasticity for two-dimensional composites, *Proc. R. Soc. Lond. A*, *438*, 531–544, 1992.

Thovert, J.-F., P. Spanne, C. G. Jacquin, and P. M. Adler, Grain reconstruction of porous media: Application to a low porosity Fontainebleau sandstone, *Phys. Rev. E*, 63061307, 2001.

Winkler, K. W., Contact stiffness in granular porous materials: Comparison between experiment and theory, *Geophys. Res. Lett.*, *10*, 1073–1076, 1983.

C. H. Arns and W. V. Pinczewski, School of Petroleum Engineering, University of New South Wales, Sydney NSW 2052, Australia. (c.arns@unsw.edu.au; v.pinczewski@unsw.edu.au)

M. A. Knackstedt, Department of Applied Mathematics, Research School of Physical Sciences and Engineering, Australian National University, Canberra ACT 0200, Australia. (mak110@rsphysse.anu.edu.au)